frontiers | Frontiers in Marine Science

TYPE Original Research
PUBLISHED 09 April 2024
DOI 10.3389/fmars.2024.1305495

OPEN ACCESS

EDITED BY
Haruko Kurihara,
University of the Ryukyus, Japan

REVIEWED BY
Matthew John Harke,
Gloucester Marine Genomics Institute (GMGI), United States
Michael William Lomas,
Bigelow Laboratory For Ocean Sciences, United States
Hisashi Endo,
Kyoto University, Japan

*CORRESPONDENCE
Mark E. Warner
mwarner@udel.edu

RECEIVED 01 October 2023
ACCEPTED 26 March 2024
PUBLISHED 09 April 2024

CITATION
Vidyarathna NK, Smith LE, Miller KR, Coyne KJ, Cohen JH and Warner ME (2024) Short-term and long-term exposure to combined elevated temperature and CO_2 leads to differential growth, toxicity, and fatty acid profiles in the harmful dinoflagellate *Karlodinium veneficum*. *Front. Mar. Sci.* 11:1305495. doi: 10.3389/fmars.2024.1305495

Short-term and long-term exposure to combined elevated temperature and CO_2 leads to differential growth, toxicity, and fatty acid profiles in the harmful dinoflagellate *Karlodinium veneficum*

Nayani K. Vidyarathna[1,2], Laura E. Smith[1,3], Katherine R. Miller[4], Kathryn J. Coyne[1], Jonathan H. Cohen[1] and Mark E. Warner[1]*

[1]College of Earth, Ocean and Environment, School of Marine Science and Policy, University of Delaware, Lewes, DE, United States, [2]Horn Point Laboratory, University of Maryland Center for Environmental Science, Cambridge, MD, United States, [3]Department of Microbiology, The University of Tennessee, Knoxville, TN, United States, [4]Department of Chemistry, Henson School of Science and Technology, Salisbury University, Salisbury, MD, United States

Ocean warming and acidification may significantly alter the distribution and intensity of harmful algal blooms as well as their effects on marine food webs. Estimating such effects rely, in part, on understanding the physiological response of individual algal species to controlled laboratory simulations of climate change conditions. Here we report the physiological response of the harmful dinoflagellate *Karlodinium veneficum* to the combined effects of elevated temperature and CO_2 (29°C/1000 ppm CO_2). We first examined these effects by comparing ambient control (25°C/441 ppm CO_2) and elevated conditions under short-term (~20 generations) growth. Next, we compared the short-term elevated condition to a longer-term (~200 generations) growth scenario under the same elevated temperature and CO_2. Under the short-term elevated conditions, *K. veneficum* growth declined, cell toxicity increased, and saturated and mono-unsaturated fatty acid (FA) composition varied significantly from ambient conditions. Meanwhile, after ~ 200 generations of growth under elevated temperature and CO_2, *K. veneficum* carbon assimilation, growth, and cell toxicity were significantly higher than the short-term elevated treatment. Further, while total saturated FA declined, essential fatty acids increased and likely represented an adaptive temporal response to long-term exposure to high temperature and CO_2. Such shifts in FA profiles and cell toxicity may possibly alter *K. veneficum* nutritional quality as prey and its mixotrophic behavior, thereby affecting the energy and mass transfer through the marine food webs as well as bloom dynamics.

KEYWORDS

ocean acidification, climate change, harmful algae, *Karlodinium veneficum*, algal toxicity, fatty acids, trophic transfer

1 Introduction

With the continued release of greenhouse gases, the upper ocean has warmed by 0.11°C per decade from 1971–2010, and the surface ocean pH has decreased by 0.1 since the beginning of the industrial era (IPCC, 2014, 2021). It is virtually certain that ocean warming and acidification will continue beyond 2100 (IPCC, 2014, 2021). These changes directly and indirectly affect phytoplankton physiology and their role in several marine ecosystems. How climate change could affect phytoplankton that cause harmful algal blooms (HABs) is particularly concerning because of their negative effects on aquatic ecosystems, and their impacts to socio-economics, as well as human health and wellbeing.

Over the past several decades, there is mounting evidence that climate change has increased HAB intensity, frequency, and range (Hallegraeff, 2010; Wells et al., 2015; Gobler et al., 2017; Trainer et al., 2019; Glibert, 2020; Gobler, 2020), and toxic dinoflagellate blooms are often projected to increase under future climate change scenarios (Tatters et al., 2013a; Glibert et al., 2014; Hattenrath-Lehmann et al., 2015; Gobler et al., 2017; Brandenburg et al., 2019; Glibert, 2020). However, dinoflagellate growth and cell toxicity do not always increase in response to ocean warming and/or acidification. For example, elevated CO_2 and temperature (750-1000 ppm and +4-5°C), led to increased growth and saxitoxin content in *Alexandrium catenella* (Tatters et al., 2013a), but did not affect the growth and/or the amount of brevetoxin in *Karenia brevis* (Errera et al., 2014). In addition to species-specific differences, there may be considerable variation to warming and acidification among individual genotypes within a single species. For example, elevated CO_2 and temperature exposure led to strain-specific differences in growth in eight isolates of the dinoflagellate *Alexandrium ostenfeldii*, while total toxin production remained unchanged in most strains (Kremp et al., 2012). Furthermore, toxicity responses to elevated CO_2 and temperature across dinoflagellate taxa may vary due to underlying metabolic pathways (Brandenburg et al., 2019).

Ocean warming and acidification may significantly alter phytoplankton cell biochemistry, and in particular lipid composition. Algal fatty acids, especially omega-3 long chain polyunsaturated fatty acids (n-3 LC-PUFA) such as eicosapentaenoic acid (EPA; 20:5n-3) and docosahexaenoic acid (DHA; 22:6n-3) are germane since they are exclusively synthesized by phytoplankton and are predicted to decline in response to ocean warming (Hixson and Arts, 2016) and acidification (Meyers et al., 2019). Lipid profile adjustments are also taxon-specific (Hixson and Arts, 2016) and do not always change under elevated CO_2 (Wang et al., 2017). Mesozooplankton (e.g., copepod) growth and life history, such as fecundity, egg hatching, and naupliar survival, are critically dependent on algal-derived fatty acids, and n-3 fatty acids in particular. In addition, shifts in phytoplankton fatty acid content strongly affect not only organismal fitness, but also trophic energy transfer efficiency among phytoplankton and zooplankton (Jónasdóttir et al., 2009; Cripps et al., 2016; McLaskey et al., 2019; Meyers et al., 2019).

Many experiments designed to test the effects of climate change to phytoplankton are short-term, typically lasting less than 15 algal generations (e.g. Fu et al., 2010; Errera et al., 2014; Hennon et al., 2017; Bercel and Kranz, 2019; Seto et al., 2019). However, some longer experiments have provided nuanced and unique insights into phytoplankton physiological acclimation and/or adaptation to future climate change that deviate from shorter duration experiments (e.g. Collins and Bell, 2004; Flores-Moya et al., 2012; Tatters et al., 2013b). For example, after growing diatoms for 2 years under elevated temperature (30°C), essential fatty acids that significantly declined when shifted from 26°C to 30°C for only seven days partially recovered after the longer growth period (Jin et al., 2020).

Karlodinium veneficum is a common coastal estuarine toxic dinoflagellate with a near-global distribution that produces a suite of toxic compounds called karlotoxins (KmTx) that have cytotoxic, ichthyotoxic, hemolytic, and grazer deterrent properties (Deeds et al., 2002; Adolf et al., 2007; Waggett et al., 2008; Fu et al., 2010; Place et al., 2012). *Karlodinium veneficum* blooms often cause massive fish kills and are also toxic to oyster embryos, larvae, and juveniles (Adolf et al., 2007; Glibert et al., 2007; Brownlee et al., 2008; Stoecker et al., 2008; Waggett et al., 2008). As a mixotroph, *K. veneficum* bloom initiation is affected not only by the availability of nutrients but also by prey (Adolf et al., 2008; Li et al., 2015; Lin et al., 2018). Temperature, light intensity, and dissolved inorganic carbon availability also affect growth (Adolf et al., 2007, 2009; Fu et al., 2010). *Karlodinium veneficum* growth is often greater at an intermediate temperature (e.g., 25°C) than at slightly warmer temperatures (e.g., 28–30°C; Lin et al., 2018; Vidyarathna et al., 2020, 2023), and is also resilient to low pH (7.8–6.0; Nielsen et al., 2010), and increases at high pCO_2 (e.g., 745 ppm) (Fu et al., 2010). In addition, high temperature (i.e. ≥ 28°C) or high pCO_2 can increase *K. veneficum* cell toxicity (Fu et al., 2010; Vidyarathna et al., 2020), but these factors were treated in isolation and under short-term exposure. In this regard, it is unclear how the combined effects of elevated temperature and CO_2 may affect *K. veneficum* physiology and long-term acclimation or adaptation.

Here, we tested the physiological response of a mid-Atlantic strain of *Karlodinium veneficum* to short- and long-term growth under combined warming and acidification. Our central objective was to compare growth, photosynthesis, cellular biochemistry, and toxicity after short-term (~20 generations, 40 days) and long-term exposure (~200 generations, 380 days) to projected future high temperature and CO_2 conditions. Long-term treatments resulted in greater growth, toxicity and essential fatty acids than in short-term treatments thereby providing potential implications for both *Karlodinium* prey and its predators.

2 Materials and methods

2.1 General experimental design

Short-term experiments were conducted at two temperatures and CO_2 concentrations: 'ambient' conditions were set as 25°C and 400 ppm pCO_2, while the 'treatment' conditions were designed to simulate warming and acidification conditions projected for the end of the 21st century (baseline RCP scenarios, IPCC, 2014) and set to 29°C and 1000 ppm pCO_2. Cultures were acclimated to short-term ambient and treatment conditions for at least 20 generations in

steady state before examining the short-term response (abbreviated as ST hereafter) to elevated temperature and CO_2. The treatment cultures were then further acclimated for ~200 generations to measure if the long-term (abbreviated as LT hereafter) response to elevated temperature and CO_2 differed from the ST response to these same conditions.

2.2 Phytoplankton cultures and acclimation to experimental conditions

Karlodinium veneficum, originally collected from the Delaware Inland Bays, Delaware, USA (CCMP2936; National Center for Marine Algae and Microbiota, Bigelow, USA), was initially grown in replicate (n=4) non-axenic batch cultures in modified f/2 media (320 µM NO_3^- and 20 µM PO_4^{3-}; Guillard and Ryther, 1962) at 25°C under a light intensity of 100 µmol photons m^{-2} s^{-1} provided by cool white fluorescent bulbs set to a 12:12 hour light:dark cycle. Media seawater was collected from the Indian River Inlet, DE, diluted with laboratory-grade fresh water to a salinity of 20, and the total alkalinity was adjusted to ~2200 µmol kg^{-1} by adding $NaHCO_3$. This TA adjustment was done to avoid disrupting the carbonate chemistry of the stock cultures and to bring the carbonate chemistry parameters back to the baseline level since the dilution reduced the DIC and TA significantly (~1000 and ~800 umol kg-^{1} for TA and DIC respectively). Water was then filtered (0.2µm, Whatman Polycap 75 TC) and autoclaved. Algal cultures were slowly acclimated to aeration by bubbling filtered (0.2 µm) air through fine glass frits (Prism Research Glass Inc., USA), and were kept in log-phase growth by weekly inoculations into fresh f/2 media.

Cultures were then transferred to 2L Pyrex bottles (Corning) and maintained in temperature- and pH-controlled cyclostats, containing filter-sterilized media (n=4, 25°C, 400 ppm pCO_2) under the same light conditions as described above (see MacIntyre and Cullen (2005) for detailed description of continuous algal culturing). Cultures were sampled every two days to monitor cell growth by cell number and *in vivo* chlorophyll *a* (chl *a*) fluorescence. The media inflow rate was adjusted to match the intrinsic growth rate of acclimated cultures (based on cell number) until cultures reached steady state (~3 weeks) and was held constant through the rest of the experimental period. Steady-state conditions were confirmed when cell density and *in vivo* chl *a* fluorescence no longer changed during the acclimation phase and for several days after inflow rate adjustments stopped. Once cultures were fully acclimated to the ambient conditions, they were grown for a further ~18 generations (40 days) in pH-controlled continuous culture.

Treatment batch cultures were initially acclimated to 29°C by ramping the temperature at a rate of 0.5°C day^{-1} in temperature-controlled incubators (Percival Scientific), and were held for ~6 generations prior to transferring to pH-controlled cyclostats. For elevated temperature conditions, cyclostat bottles were kept in a clear acrylic water jacket connected to a recirculating water bath set to 29°C. The pCO_2 in each bottle was then slowly raised to ~1000 ppm at a rate of 100 ppm day^{-1}. Cell growth was regularly monitored after the pCO_2 ramping period, and the media inflow rate was adjusted to match the intrinsic growth rate as explained above for ambient cultures. To limit biofouling, cultures were transferred to new sterile bottles every three weeks. Short-term (ST) treatment conditions lasted for ~22 generations (58 days) after which cultures were sampled for physiological analyses. The remaining cultures were further acclimated to treatment conditions for an additional ~180 generations. After ~200 generations at steady state (381 days total), treatment cultures were considered acclimated to long-term (LT) conditions and were sampled again for physiological analyses. All routine samples (i.e., prior to terminating an experiment) for biomass estimation and carbonate chemistry parameter analyses were withdrawn directly from the cultures using a sample tube attached to the culture vessel.

2.3 Carbonate chemistry control and measurement

CO_2 levels (~400 and 1000 ppm) were controlled with a pH-stat system (Qubit Systems Inc, Canada), with pH levels set to 8.2 and 7.9 for ambient and treatment conditions respectively. The pH in each culture bottle was continually recorded and logged in computer-controlled software (Logger Pro) that controlled a 3-way solenoid delivering either CO_2 (certified 2%, Tech Gas Inc, USA) or CO_2-free air passed through a soda lime column. pH electrodes were cleaned and re-calibrated with NBS buffer standards (pH 4.01 and 9.18, Orion™) every 7-14 days. The pH stability and accuracy of the system was confirmed by independent measurements of culture outflow with a laboratory grade pH system (Fisher Scientific A815 Plus pH meter equipped with Fisherbrand™ accumet™ pH sensor).

The total dissolved inorganic carbon (DIC) of each container was analyzed using an in-house custom DIC analyzer (Friedrich et al., 2002). Water samples were acidified, followed by gas stripping and delivery to a non-dispersive infrared gas analyzer (LI-Cor) for total CO_2 measurement. Media and sample total alkalinity (TA) were measured using a bromocresol purple colorimetric assay (Yao and Byrne, 1998) with a spectrometer (Ocean Optics, USB4000-ES) and a titrator (Metrohm 876 Dosimat plus, Switzerland). All DIC and TA measurements were compared to certified reference materials (Dickson laboratory, San Diego, USA), and seawater carbonate chemistry was calculated with the CO2SYS software (Pierrot et al., 2006) based on DIC and pH (NBS) (Table 1).

2.4 Cell growth and chlorophyll a

Cell growth was monitored every two days by measuring *in vivo* chl *a* fluorescence (10 AU; Turner Designs, USA) and active chl *a* fluorescence (fast repetition rate fluorometry, Chelsea Instruments, UK), and periodic cell counts confirmed estimates by *in vivo* fluorescence. Cell density was calculated by counting glutaraldehyde-preserved (final concentration 1% v/v) sub samples (1 mL) with a Neubauer hemocytometer and a light microscope (100x magnification). Chl *a* concentration was determined according to Welschmeyer (1994), with acetone

TABLE 1 Seawater carbonate chemistry parameters for ambient and treatment conditions.

	Ambient	Treatment
DIC (µmol kg^{-1})	2156 ± 99 (44)	2577 ± 135 (84)
pH (NBS)	8.33 ± 0.17 (40)	7.92 ± 0.13 (64)
Total Alkalinity (µmol kg^{-1})	2371 ± 112 (44)	2727 ± 132 (73)
pCO_2 (µatm)	441 ± 29 (44)	1084 ± 64 (76)

Values are mean ± SD, with replicate number for each parameter in parentheses.

extracts measured on a fluorometer (10 AU; Turner Designs, USA). Once cultures reached steady-state, cell biomass was monitored several times each week by *in vivo* chl *a* fluorescence. Cell specific growth rate (µ, day^{-1}) was calculated according to Brading et al. (2011), using the following formula:

$$\mu = \frac{\ln\left(\frac{C_{t+\Delta t} \times Vol_{t+\Delta t}}{C_t \times Vol_t}\right) + \left(\frac{Vol_{waste}}{Vol_{vessel}}\right)}{\Delta t} \quad (1)$$

where t = time (days), Δ t = time interval between sampling, C = *in vivo* chl *a* fluorescence, Vol = culture volume in the vessel at the time of sampling, Vol_{waste} = outflow volume (mL) generated during the time interval between sampling and Vol_{vessel} = the maximum volume of medium (mL) in the vessel.

2.5 Cell photochemistry

Cells were dark acclimated for 15 min and algal photochemistry was monitored by active chl *a* fluorescence by fast repetition rate fluorometry (FRRf) with a FASTtracka II fluorometer with a FASTact light and temperature control assembly (Chelsea Instruments, UK) connected to a constant temperature water bath set to the growth temperature. Fluorescence induction was recorded by applying a single-turnover fluorescence protocol that consisted of 100 1µs flashlets at ~1-µs intervals provided by a bank of blue LEDs (peak excitation 450 nm, 200 µs total induction time), followed by 50 flashlets spaced at increasing intervals to allow for PSII reaction center re-oxidation. Measurements were recorded from the average of 15–30 acquisitions at 100 ms intervals. Photochemical activity in the light activated state was then assessed by the same fluorescence induction protocol after exposing cells to white light for 3 min that was provided by a bank of LEDs set to 104 µmol photons m^{-2} s^{-1}. Fluorescence data were fit in FASTpro software (v3.0, Chelsea Instruments) and used to calculate the maximum quantum yield of photosystem II (F_v/F_m) and the quantum yield of photosystem II in the light activated state (F_q'/F_m') (Cosgrove and Borowitzka, 2010).

2.6 Photosynthetic carbon assimilation

Subsamples were removed from each replicate culture (5 mL) and combined with 12.5 µL of ^{14}C sodium bicarbonate (specific activity 0.1 µCi mL^{-1} MP Biomedicals) and incubated in a temperature-controlled aluminum block set to 25°C or 29°C for 30 min. Light in each well was set to 200 µmol photons m^{-2} s^{-1} and was provided by a cool white LED under each sample well. Preliminary measurements confirmed that photosynthesis in all samples was saturated at this light intensity (average E_k ~ 160 µmol photons m^{-2} s^{-1}). Dark controls were run in duplicate. Incubations were stopped by adding 1% glutaraldehyde (final concentration) to each vial, and residual inorganic C was removed by adding hydrochloric acid (1.2 M final concentration), followed by shaking samples overnight. After adding 5 mL scintillation cocktail (Ultima Gold, Perkin Elmer), radioactivity was measured in a liquid scintillation counter (Beckman LS-6500). Carbon assimilation in the light was corrected for any dark incorporation and expressed as the assimilation rate normalized to cell number (cell h^{-1}). As samples were not filtered after ^{14}C assimilation, presented values include both particulate and dissolved production.

2.7 Particulate organic carbon, nitrogen and phosphorus

Samples (25-50 mL) for particulate organic carbon (POC), nitrogen (PON) and phosphorus (POP) were filtered onto 25 mm pre-combusted glass-fiber filters (2h at 450°C, GF/C, Whatman), dried at 60°C for 24 h, and then stored in a desiccator prior to analyses. Cellular C and N were quantified with a CHN elemental analyzer (ECS 4010 Elemental combustion system; Costech Instruments, USA), with phenylalanine and EDTA used as standards. POP was measured following the method of Solórzano and Sharp (1980) using Phosphate standard (RICCA, 1000 ppm PO_4^{3-}).

2.8 Carbohydrates and soluble proteins

Twenty-five to fifty milliliter samples were centrifuged (4,800 x g) and cell pellets were stored at -20°C until further analyses. Carbohydrate content was determined by the phenol-sulphuric acid method using D-(+)-glucose as a standard (DuBois et al., 1951) after acid hydrolyzing the cell pellets in 1M H_2SO_4 at 100°C for 1 h. Proteins were extracted by bead beating (BioSpec) cell pellets with 0.5 mm glass beads for 60 s in 500 µL of filtered sea water (FSW, nominal pore 0.2 µm) followed by centrifugation (3,380 x g, 5 min). Soluble protein was determined with a linearized Bradford assay (Ernst and Zor, 2010). All absorbance measurements were recorded using a plate reader (FLUOstar Omega, BMG Labtech).

2.9 Fatty acids

Fifty milliliter samples were centrifuged (4,800 x g) and the pellets were freeze-dried (Virtis, 12SL) and stored in a desiccator. Prior to lipid extraction, samples were spiked with 20 µL of C13:0ME internal standard (10 mg mL^{-1}, Sigma Aldrich, St. Louis, MO). Acid-catalyzed transesterification of lipids to fatty acid methyl esters (FAMEs) and the extraction of FAMEs into hexane was performed as in Van Wychen et al. (2013). FAME extracts were stored at -20°C until analysis. Supelco 37 Component FAME mix (Sigma Aldrich, St.

Louis, MO) was spiked with the 5 µL of the same C13:0ME internal standard as above and were used as standards (total fatty acid concentration ranging from 0.01 to 0.5 mg mL^{-1}). FAMEs were analyzed by gas chromatography (GC) on a Hewlett Packard HP 7890B Series (Palo Alto, CA) equipped with a flame ionization detection and a Zebron ZB-1 wax column (30m x 250µm x 25µm, Phenomenex, Torrance, CA). FAMEs were separated using splitless injection (injection volume =3 µL, inlet temperature = 250°C). An initial column heating to 100°C was maintained for 1 min followed by ramping at 25°C min^{-1} up to 170°C, then 2°C min^{-1} up to 200°C, which was held for 1 min prior to ramping at 18°C min^{-1} up to 250°C, which was held for 8 min. FAMEs were identified based on their retention times, and peaks were compared to the standard curve in Open LAB CDS GC software (Agilent Technologies). Fatty acid recovery was corrected for the recovery of the internal standard, and FAME concentration normalized to cell number was then converted to the corresponding fatty acid concentration using individual Sheppard factors (Sheppard, 1992).

2.10 Cellular toxicity

Fifty milliliter samples were centrifuged (4,800 x g) at 4°C (Sorval RC-5B, USA), and cell pellets were extracted in 1–2 mL of methanol for 24 h in the dark at -20°C. Cell toxicity was assessed by the hemolytic assay according to Eschbach et al. (2001) and with a Rainbow Trout (RT) fish gill cell (FGC) assay according to Dayeh et al. (2005) with modifications (Vidyarathna et al., 2020) and was normalized to total cellular carbon.

2.11 Data analyses

Statistical analyses were performed using R (v 4.1.1; R Core Team 2021). The data were checked for normality and homogeneity of the variance by Shapiro-Wilk and Bartlett tests respectively. Treatment effects (increased temperature and CO_2) were tested between ambient and ST cultures and the effect of acclimation time to increased temperature and CO_2 (short term and long term) between ST and LT cultures were analyzed separately using one-way analysis of variance (ANOVA). Results were considered significant at $\alpha = 0.05$.

3 Results

3.1 Cell growth, carbon assimilation, photophysiology and chlorophyll *a*

The ambient cell growth rate was 0.32 ± 0.02 day^{-1}, while the treatment growth significantly decreased in the short-term (ST) cultures to 0.27 ± 0.01 (ANOVA, p=0.006, on day 50); however, after ~200 generations, growth in the long-term (LT) treatment increased to 0.36 ± 0.01 day^{-1} (ANOVA, p=0.0004 compared to ST cultures, Figure 1). Carbon assimilation on the other hand increased in response to both treatment effect (ANOVA, p= 0.03 between ambient and ST cultures) and to acclimation time (ANOVA, p= 0.03 between ST and LT cultures) (Figure 2). In contrast, ambient *K. veneficum* cultures had a higher PSII maximum quantum yield (*Fv/Fm*), than the ST cultures (ANOVA, p= 0.0004, Figure 3A). Of the two treatments, *Fv/Fm* was significantly higher in the LT cultures than in the ST cultures (ANOVA, p=0.01). There was less variability in the effective quantum yield of PSII (F_q'/F_m') in the light activated state (Figure 3B), as F_q'/F_m' was significantly lower in the ST cultures than in the ambient and LT cultures (ANOVA, p=0.02 and 0.005, respectively). Overall, *Fv/Fm* and *Fq'/Fm'* ranged between 0.44-0.48 and 0.39-0.41 respectively, and no warming or acidification induced stress on *K. veneficum* photochemistry was evident. Cellular chl *a* remained unchanged between ambient and ST cultures (ANOVA, p=0.16) and increased significantly in LT cultures compared to ST cultures (ANOVA, p<0.001, Figure 3C).

3.2 Elemental composition and cellular carbohydrates and proteins

Cell quotas for C and P (POC and POP) were not affected by treatment (ANOVA, p= 0.08 and 0.73 for POC and POP respectively) or acclimation time (ANOVA, p= 0.40 and 0.81 for POC and POP respectively) and remained unchanged across ambient, ST, and LT cultures (Table 2). In contrast, N cell quota (PON), was significantly higher in ST cultures than in ambient cultures (ANOVA, p= 0.01), but remained unchanged between ST and LT cultures (ANOVA, p= 0.49). Meanwhile, the atomic N:P and C:P ratios remained similar across ambient and ST cultures (ANOVA, p=0.57 and 0.81 for N:P and C:P ratios respectively) and ST and LT cultures (ANOVA, p=0.94 and 0.15 for N:P and C:P ratios respectively, Table 2), while the C:N ratio was significantly lower in ST cultures than the ambient and LT cultures (ANOVA, p=0.004 and p=0.002, respectively, Table 2).

Cellular carbohydrates were significantly higher in ST cultures than in ambient cultures (ANOVA, p=0.01, Table 2), but decreased slightly in the LT cultures in comparison to the ST cultures (ANOVA, p=0.2). ST culture cellular protein was also significantly higher than both ambient (ANOVA, p=0.0007) and LT cultures (ANOVA, p=0.002, Table 2).

3.3 Cellular fatty acid composition

Total fatty acid content remained similar across each culture condition and ranged between 21-33 pg $cell^{-1}$ (ANOVA, p=0.09 and 0.99 for ambient vs. ST and ST vs. LT comparisons respectively, Figure 4A). In contrast, fatty acid composition changed considerably in response to (short-term treatment and time (Figures 4B, C). The percentage of saturated fatty acids (SFA) was higher in the ST cultures than the ambient cultures (ANOVA, p=0.0007), but this increase was not sustained through time under the treatment conditions, as SFAs decreased significantly in the LT

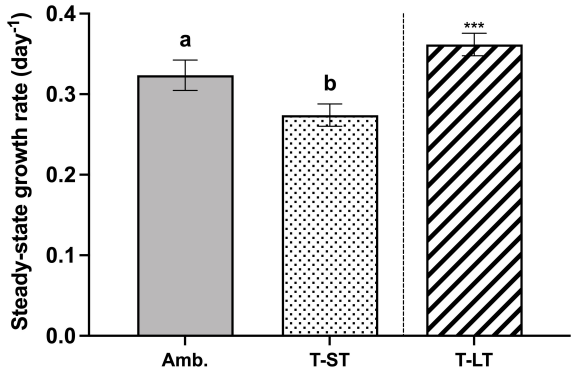

FIGURE 1
Steady-state growth rates (μ, day^{-1}) of *K. veneficum* acclimated to Ambient (Amb.) and treatment conditions (short term: ST and long term: LT). Error bars denote the standard deviation of 40, 76 and 84 replicates for Amb., ST and LT cultures, respectively. Letters above the bars indicate significant differences between ambient and ST cultures (treatment effects) while asterisks indicate significant differences between ST and LT cultures (acclimation time effect) (ANOVA, $p < 0.05$).

cultures (ANOVA, p<0.0001, Figure 4B). In contrast, the percentage of monounsaturated fatty acids (MUFA) in the ST cultures was significantly lower than the ambient cultures (ANOVA, p<0.0001), while the LT culture MUFAs were significantly higher than the ST cultures (ANOVA, p<0.0001, Figure 4B).

Polyunsaturated fatty acids (PUFA) accounted for only 2.4–8.6% of total FA content and were similar between ambient and ST (ANOVA, p=0.61), and ST and LT culture conditions (ANOVA, p=0.89, Figure 4C). However, the PUFA composition changed substantially in the LT cultures. In particular, the percentage of n3 fatty acids (n3 FA), a subgroup of PUFA, was significantly

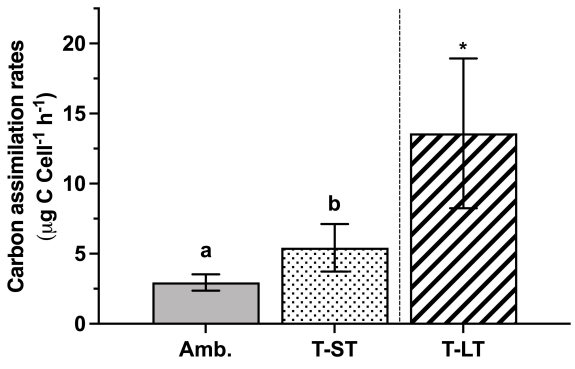

FIGURE 2
Carbon assimilation rates of *K. veneficum* (μg C Cell^{-1}, h^{-1}) acclimated to ambient (Amb.) and treatment conditions (short term: ST and long term: LT). Error bars denote the standard deviation of 4 replicates (n=4) for Amb and ST cultures and 3 replicates (n=3) for LT cultures. Letters above the bars indicate significant differences between ambient and ST cultures (treatment effects) while asterisks indicate significant differences between ST and LT cultures (acclimation time effect) (ANOVA, $p < 0.05$). Carbon assimilation rates per chlorophyll *a* (μg C Chl *a*$^{-1}$, h^{-1}) and cellular carbon (μg C C^{-1}, h^{-1}) yielded the same results (data not shown).

greater than those recorded in the ST cultures (ANOVA, p=0.0003, Figure 4C). Notably, both major essential fatty acids EPA (eicosapentaenoic acid) and DHA (docosahexaenoic acid) were significantly greater in LT cultures than in the ST cultures (ANOVA, p<0.0001, Figure 4C). We also observed an increase in the percentage of very long chain fatty acids over time (VLCFA, i.e. FA with carbon chains >20) from ~6% in ST cultures to approximately 15% in the LT cultures (Supplementary Table 1).

Twenty-seven fatty acids were identified (Supplementary Table 1), and the two most abundant SFA in *K. veneficum* were palmitic acid (16:0) and myristic acid (14:0), which together represented 66%, 76% and 45% of the total FA content at ambient, ST and LT cultures, respectively. Oleic and elaidic acids (18:1 cis+trans) together represented the major MUFA in ambient cultures, while eicosenoic acid (20:1) was the dominant MUFA in the treatment cultures. *Karlodinium veneficum* n3 PUFA included alpha-linolenic acid (ALA, 18:3n-3), eicosapentaenoic acid (EPA, 20:5n-3), and docosahexaenoic acid (DHA, 22:6n-3). In addition, eicosatrienoic acid (ETE, 20:3n-3) was also detected in the LT cultures.

3.4 Cell toxicity

Hemolytic activity normalized to either cell number or carbon remained unchanged between the ambient and ST treatment and when comparing ST vs LT conditions (ANOVA, p>0.5, Figure 5); however, toxicity against the fish gill cell (FGC) line increased (i.e., EC_{50} decreased) significantly in both ST and LT cultures (Figure 5). Specifically, the FGC toxicity in the ST cultures was 2.5 times greater than the ambient cultures (ANOVA, p=0.001), while FGC toxicity was 2.6 times greater in the LT cultures than in the ST cultures (ANOVA, p=0.005). Likewise, when normalized to cellular carbon (EC50: μg C mL^{-1}), FGC toxicity followed a similar pattern and increased significantly from ambient to ST (ANOVA, p=0.0001) and ST to LT (ANOVA, p= 0.01) culture conditions.

4 Discussion

Acclimating *K. veneficum* to long term (LT, ~200 generations) combined elevated temperature and CO_2 increased carbon assimilation, growth, and FGC toxicity. The long-term treatment also resulted in major changes in key fatty acid classes, as the percent of monounsaturated (MUFA) and essential fatty acids (n3 FA) increased, while saturated fatty acids (SFA) decreased. However, some of these differences were not evident or changed in opposite ways when *K. veneficum* was acclimated to short-term (ST, ~20 generations) elevated temperature and CO_2. For example, ST growth and % MUFA were lower and % SFA were higher than the ambient cultures, while carbon fixation remained similar in both conditions. In contrast, other cellular parameters, such as FGC toxicity, were consistently higher in ST cultures than in ambient conditions. These different results between the ST and LT experiments suggest that complete acclimation to elevated temperature and pCO_2 required >20 generations.

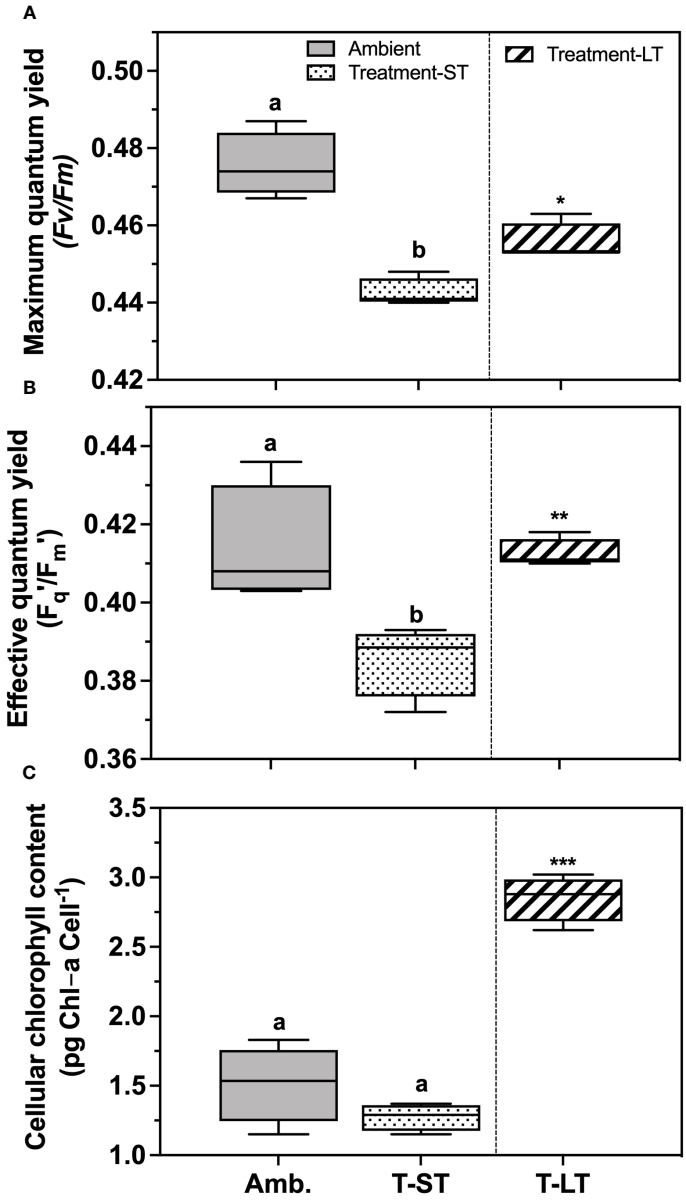

FIGURE 3
Maximum photochemical efficiency of photosystem II (*Fv/Fm*) **(A)**, effective light acclimated photochemical efficiency of PSII (F_q'/F_m') **(B)** and cellular chlorophyll-*a* content (pg Chl-*a* cell^{-1}), **(C)** of *K. veneficum* acclimated to ambient (Amb) and treatment conditions (short term: ST and long term: LT). Error bars denote the standard deviations: Amb, n=4; ST n=36 and LT, n=21 panels **(A, B)** and Amb, n=4; ST, n=4; LT, n=3 (panel **(C)**. Letters above the bars indicate significant differences between ambient and ST cultures (treatment effects) while asterisks indicate significant differences between ST and LT cultures (acclimation time effect) (ANOVA, $p< 0.05$).

4.1 The effects of combined elevated temperature and CO_2 on *K. veneficum* growth and toxicity

While our experimental design did not allow us to test the independent effects of elevated temperature and CO_2, *K. veneficum* and some other dinoflagellates often grow faster under elevated CO_2 (Fu et al., 2010; Errera et al., 2014) but grow slower under elevated temperature (Seto et al., 2019; Vidyarathna et al., 2020, 2023). However, pre-acclimation to heating prior to changing CO_2 can lead to different outcomes, as Coyne et al. (2021) noted higher growth after acclimating *K. veneficum* to 30°C for over one year prior to applying short-term high CO_2 (24 days/750 ppm CO_2). Excess CO_2 may provide this *K veneficum* isolate some relief from heating, whereby elevated CO_2 reduces the energetic demand for acquiring and fixing carbon at higher temperatures. We hypothesize that lower growth rates in the ST cultures were likely caused by a stronger negative effect of temperature than high CO_2. This may be common in many short-term experiments (typically < ~20 generations) and explains similar growth responses in this and other dinoflagellates when comparing 'combined' and 'warming only' treatments in similar experimental designs (Feng et al., 2008; Fu et al., 2008; Seto et al., 2019). Likewise, our previous work has noted that the thermal optima for growth in this strain of *K. veneficum* is closer to 25°C (Vidyarathna

TABLE 2 Cell densities, cellular carbon, nitrogen, phosphorus, elemental ratios, and cellular carbohydrate and soluble protein of *K. veneficum* acclimated to ambient, treatment-ST and treatment-LT conditions.

	Ambient	Treatment-ST	Treatment-LT
Cell density (10^4 Cells mL^{-1})	5.28 ± 0.93	10.2 ± 0.69	19.2 ± 2.5
POC (pg $Cell^{-1}$)	144 ± 21	167 ± 7.4	182 ± 33
PON (pg $Cell^{-1}$)	25 ± 4.4[a]	34 ± 2.1[b]	32 ± 5.4
POP (pg $Cell^{-1}$)	2.47 ± 0.93	2.64 ± 0.27	2.54 ± 0.79
N:P	26 ± 8.3	29 ± 2.3	29 ± 5.2
C:N	6.69 ± 0.36[a]	5.70 ± 0.23[b]	6.62 ± 0.16**
C:P	170 ± 49	163 ± 10	191 ± 31
Carbohydrates (pg $Cell^{-1}$)	17 ± 9.8[a]	64 ± 24[b]	41 ± 10
Proteins (pg $Cell^{-1}$)	13 ± 3.4[a]	29 ± 3.6[b]	14 ± 2.3**

Errors denote the standard deviations of four replicates (n = 4) for ambient and ST cultures and three replicates (n=3) for LT cultures. Superscript letters indicate significant differences between ambient and ST cultures (treatment effects) and asterisks indicate significant differences between ST and LT cultures (acclimation time effect) (ANOVA, $p< 0.05$).

et al., 2020). While carbon fixation remained similar between the ambient and ST treatment, the lower photochemical performance in the ST treatment (Figures 3A, B) that was not apparent in the LT treatment suggests that some aspect of photosynthetic electron transport in the light reactions may have been the rate limiting step in the ST acclimation. Although not evaluated in our study, the possible shifts in bacterial consortia [e.g. *Alteromonas* (Deng et al., 2022)] associated with *K. veneficum* cultures may also have contributed to promoting algal growth under elevated temperature and CO_2 as has been reported for other photosynthetic organisms such as *Prochlorococcus* (Hennon et al., 2018).

While growth was higher in the LT treatment, carbon assimilation still exceeded the growth rate while elemental composition remained unchanged. Such decoupling between photosynthesis and growth may signal a mechanism to remove excess photosynthate as dissolved organic carbon, perhaps as transparent exopolymeric particles (Engel et al., 2014; Passow and Laws, 2015), when electron transport and carbon fixation are high (Claquin et al., 2008). In contrast, when exposed to long term high CO_2 (~900 generations), the diatom *Phaeodactylum tricornutum* reduced photosynthesis and respiration, thereby allocating a similar amount of carbon for growth as the low CO_2 selected population with no change in growth rates (Jin et al., 2022). Similar to our LT treatments, phytoplankton elemental composition, including in other dinoflagellates, does not necessarily change in response to elevated CO_2 (Burkhardt et al., 1999; Clark et al., 2014; Wynn-Edwards et al., 2014; Sugie and Yoshimura, 2016; Bercel and Kranz, 2019; Xu et al., 2023), but intracellular distributions can still change, as Chl *a* content approximately doubled in our LT treatments. In contrast, nitrogen, protein, and carbohydrate quotas increased in the ST cultures and this excess stored carbon may reflect a more immediate physiological response to elevated temperature and CO_2.

The greater *K. veneficum* FGC toxicity under elevated temperature and CO_2 noted between ambient and ST cultures as well as ST and LT cultures is similar (~ 52%) to increased FGC toxicity in this same isolate in response to elevated temperature alone, which peaked at 25°C–28°C (Vidyarathna et al., 2020). Hence, the increased FGC toxicity in our ST treatment was possibly due more to elevated temperature than CO_2. Meanwhile, the even greater increase in FGC toxicity in the LT cultures (57% higher than the ST cultures) perhaps represented further cellular adjustments to carbon allocation in response to the combined effects of elevated temperature and CO_2.

In contrast to FGC toxicity, hemolytic toxicity remained similar across ambient and the ST treatment cultures and also did not change in the LT treatment. Notably, elevated temperature alone led to increased hemolytic toxicity in late-exponential phase batch cultures of *K. veneficum*, and batch grown *K. veneficum* hemolytic toxicity $cell^{-1}$ at 25°C was 4x higher (Vidyarathna et al., 2020) than in the continuous cultures reported here. Further, although *K. veneficum* hemolytic activity increased with elevated CO_2 and P-limitation (Fu et al., 2010), the absolute toxicity $cell^{-1}$ was lower than data from batch cultures [> ~50 ng $cell^{-1}$ vs. 95 ng $cell^{-1}$ in Vidyarathna et al. (2020)]. While we cannot discount possible synergestic effects of elevated temperature and CO_2, *K. veneficum* hemolytic activity may be affected more by nutrient limitation and starvation.

4.2 Temporal changes in *K veneficum* lipids under elevated temperature and CO_2 and the possible implications for trophic transfer and mixotrophy

Phytoplankton often change their fatty acid (FA) composition to maintain membrane homeoviscocity in response to changing temperature (Sinensky, 1974). Increasing saturated fatty acid content at higher temperature helps to maintain membrane rigidity (Fuschino et al., 2011; Baker et al., 2018; Hixson and Arts, 2016), which we also noted in our ST treatment. However, not all shifts in FA content in our ST treatment were similar to previous studies where the % PUFA often declines at higher temperature (Fuschino et al., 2011; Hixson and Arts, 2016; Torstensson et al., 2013; Hyun et al., 2016) but remained unchanged here. Further, while FA composition (% SFA and MUFA) did not change in phytoplankton within mesocoms exposed to elevated temperature and CO_2 for 20 days (Meyers et al., 2022), we found a significant decrease in the % MUFA in our ST treatment. Hence, *K. veneficum* FA reaction norms may change rapidly in response to both elevated temperature and CO_2 but are likely species- and strain- dependent (Jin et al., 2020) and not necessarily reflective of the larger phytoplankton community.

In contrast to the ST cultures, the significant increase in growth and decline in total saturated FA in the LT cultures may have been an adaptive response; however, our experimental design did not have a long-term ambient control to directly compare against the LT treatment. Furthermore, this also prevented us from explicitly testing for trait adaptation by performing reciprocal shifts between

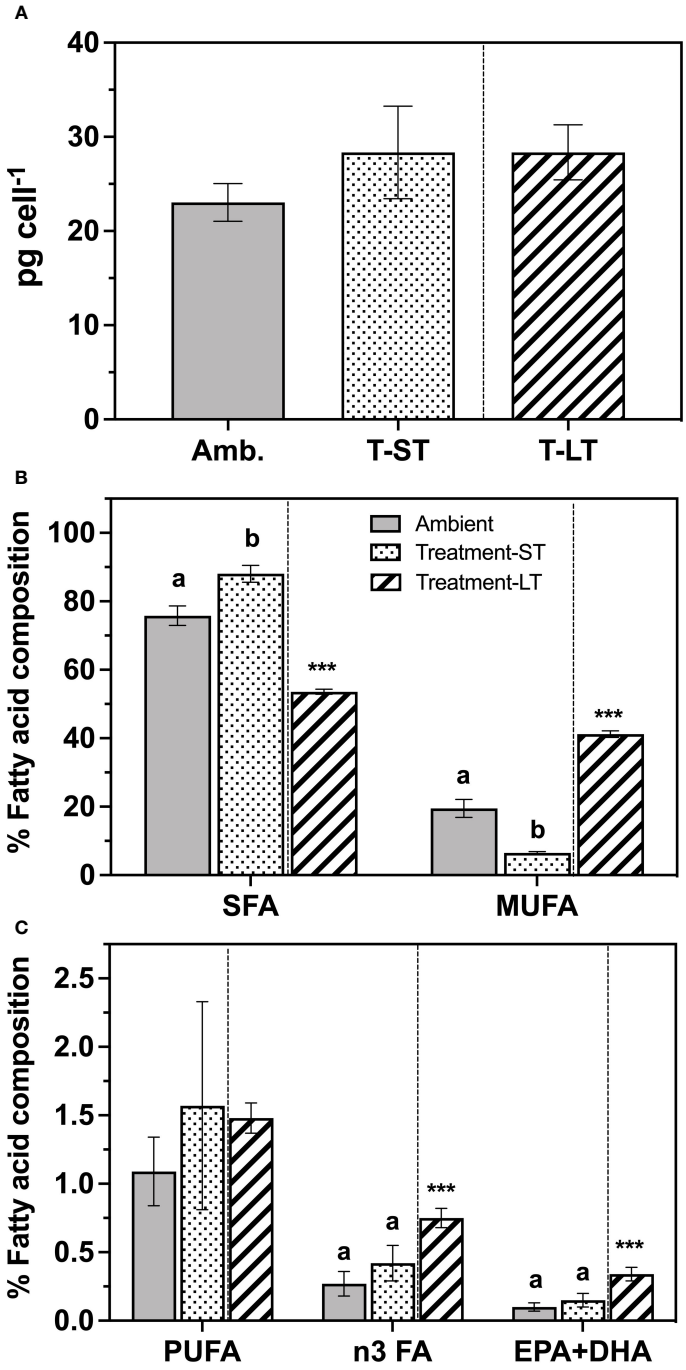

FIGURE 4
Total fatty acid contents (pg cell^{-1}) **(A)**, and percent composition of saturated fatty acids (SFA), mono-unsaturated fatty acids (MUFA) **(B)**, and polyunsaturated fatty acids (PUFA) **(C)** of *K. veneficum* acclimated to ambient (Amb) and treatment conditions (short term: ST and long term: LT). Error bars denote the standard deviation of 4 replicates (n=4) for Amb and ST cultures and 3 replicates (n=3) for LT cultures. Letters above the bars indicate significant differences between ambient and ST cultures (treatment effects) while asterisks indicate significant differences between ST and LT cultures (acclimation time effect) (ANOVA, $p < 0.05$). n3 FA, omega-3 fatty acids; EPA, Eicosapentaenoic acid; DHA, Docosahexaenoic acid.

ambient and treatment conditions (i.e., comparing high temperature and CO_2 treated algae against the ambient control samples after shifting them into the high temperature and CO_2 and vice versa) (Schlüter et al., 2014). Nevertheless, the decline in saturated FA is similar to that noted in the diatom *Thalassiosira pseudonana*, where saturated FA were lower after 500 generations at 31°C, providing evidence for some thermal adaptation (O'Donnell et al., 2019). Importantly, the measured response traits in long-term experiments can return to pre-exposure levels or fall below those of the original non-adapted population (Schlüter et al., 2016; Collins et al., 2020). For example, initial FA and lipids declined in three diatom species and then fully recovered after two years of long-term

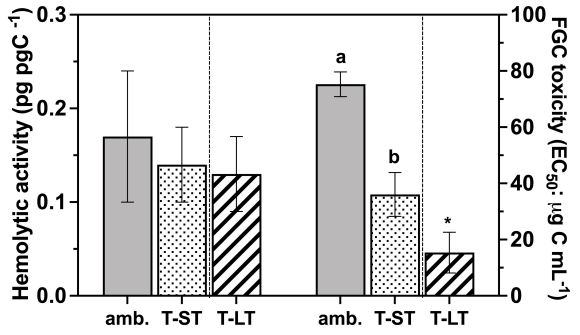

FIGURE 5
Hemolytic activity (pg pg C^{-1} - Left Y axes) and the rainbow trout fish gill cell toxicity (FGC; EC_{50}: µg Carbon mL^{-1} - Right Y axes) of *K. veneficum* acclimated to ambient (Amb) and treatment (short term: ST and long term: LT) conditions. Error bars denote the standard deviation of four replicates (n=4) for Amb and ST cultures and three replicates (n=3) for LT cultures. Letters above the bars indicate significant differences between ambient and ST cultures (treatment effects) while asterisks indicate significant differences between ST and LT cultures (acclimation time effect) (ANOVA, $p< 0.05$).

growth at 30°C (Jin et al., 2020). However, the FA profile shift in our LT cultures was a significant re-arrangement in lipid composition that included a larger proportion of essential FA and very long chain FA (VLCFA) not seen in the ST cultures. Furthermore, n-3 PUFA and n-6 PUFA increased in LT cultures (Figure 4C; Supplementary Table 1) and contrasts with the suggestion that global heating alone could favor phytoplankton n-6 PUFA over n-3 PUFA (Hixson and Arts, 2016). Hence, the increased FA elongation and desaturation in *K. veneficum* in response to long-term exposure to elevated temperature and CO_2 may represent a unique interactive effect of these combined climate stressors.

Altered algal fatty acid (FA) profiles due to climate change has important ecological implications for marine food webs, as primary consumers acquire most FA through phytoplankton grazing. While total FA content remained unchanged, elevated temperature and CO_2 led to major changes in key *K. veneficum* FA classes. Studies with other algal species have reported a broad range of FA variability from little to no change (e.g. Fitzer et al., 2019; O'Donnell et al., 2019; Meyers et al., 2022) to a significant decline in response to elevated temperature and/or CO_2 (Rossoll et al., 2012; Hyun et al., 2016; Jacob et al., 2017). Increased essential fatty acids, including EPA, DHA, in the LT treatment holds particular ecological relevance as they are exclusively synthesized by phytoplankton and affect both consumer growth and fitness. Declining phytoplankton n3 FA in response to elevated temperature potentially weakens energy and mass transfer through the marine food web (Fuschino et al., 2011; Rossoll et al., 2012; Fitzer et al., 2019; Meyers et al., 2019) where a temperature increase of 2.5°C may reduce phytoplankton EPA by 8.2% and DHA by 27.8% (Hixson and Arts, 2016). In contrast, we found a consistent increase in the percentage of n3-PUFA when moving from ambient to ST and ST to LT treatments. Additionally, since the total FA cell^{-1} did not change, the increased n3-PUFA may have resulted from desaturating pre-existing fatty acids–a process that requires reducing power from NADPH or NADH (Sato et al., 2003). Here, n3-PUFA increased proportionally with photosynthetic C fixation across ambient and treatment cultures (Figure 4), hence excess energy not used for growth may have been used to support desaturation of SFA to n3-FA.

Altered biochemical composition of algal prey can affect the growth, reproduction, survival, and biochemical stoichiometry of grazers such as copepods and bivalves (Rossoll et al., 2012; Cripps et al., 2016; Fields et al., 2022; Pan et al., 2023), and leads to cascading effects to fitness at higher trophic levels. For example, Cripps et al. (2016) estimated that at elevated CO_2, carbon trophic transfer efficiency from phytoplankton to copepods declined to <50% of the control population. However, other studies have reported greater fitness in the copepod, *Calanus finmarchicus* when raised at elevated CO_2 (Fields et al., 2022) and copepod biomass (particularly in smaller size classes) can increase at elevated CO_2, likely due to indirect effects through increased food availability (e.g. Taucher et al., 2017). In contrast, others have reported that ocean acidification alone or, in combination with elevated temperature, did not affect prey or zooplankton FA composition (Meyers et al., 2022). While these responses are results of a complex interplay of trophic interactions, short-term acclimation vs long-term adaptation as well as differences in sensitivities to elevated temperature and/or CO_2 among different taxa may explain some of this variability (Lohbeck et al., 2012; Tatters et al., 2013b; Bermúdez et al., 2015; Jin et al., 2020; Xu et al., 2023). Among the order Gymnodiniales, *Karlodinium* species are globally prevalent (Le Bescot et al., 2016), and *K. veneficum* is a common constituent in coastal mid-Atlantic waters such as the Chesapeake Bay (Zhang et al., 2008). Further, given that *K. veneficum* is consumed by micrograzers, including other heterotrophic dinoflagellates in this region (Johnson et al., 2003) as well as the copepod *Acartia tonsa* (Hong et al., 2012), possible shifts in algal biochemical composition under future warming and acidification as shown here could affect such trophic interactions.

In addition to autotrophy, mixotrophic feeding by *K. veneficum* can significantly increase bloom formation (Li A. et al., 2001; Place et al., 2012; Li et al., 2015). While not included in our experimental design, mixotrophy could play an important role in some climate change scenarios, especially in regard to elevated temperature, which can significantly increase prey ingestion and digestion (Li A. et al., 2001; Wilken et al., 2013; Li et al, 2022). Other factors related to bloom progression, such as nutrient starvation, can negatively affect algal response to pH-induced stress, and are important to consider in future studies, as mixotrophic phytoplankton may be favored under some ocean acidification scenarios (Flynn et al., 2015). Taken together our results suggest that elevated CO_2 and temperature can enhance carbon assimilation and increase *K. veneficum* autotrophic growth and toxicity, which could further influence bloom formation and severity. However, long-term exposure to these conditions also resulted in notable shifts in greater proportions of essential fatty acids that might counteract the negative effects of elevated cell toxicity to grazers. Such interactions, as well as possible shifts in mixotrophic behavior and subsequent changes to algal toxicity warrant further investigation in more complex future climate change simulations.

Data availability statement

The raw data supporting the conclusions of this article will be made available by the authors, without undue reservation.

Ethics statement

Ethical approval was not required for the studies on animals in accordance with the local legislation and institutional requirements because only commercially available established cell lines were used.

Author contributions

NV: Conceptualization, Data curation, Formal analysis, Investigation, Methodology, Visualization, Writing – original draft, Writing – review & editing. LS: Investigation, Writing – review & editing. KM: Investigation, Resources, Writing – review & editing. KC: Conceptualization, Funding acquisition, Resources, Writing – review & editing. JC: Conceptualization, Funding acquisition, Resources, Supervision, Writing – review & editing. MW: Conceptualization, Funding acquisition, Methodology, Project administration, Supervision, Writing – original draft, Writing – review & editing.

Funding

The author(s) declare financial support was received for the research, authorship, and/or publication of this article. This study was supported by the National Oceanic and Atmospheric Administration (NOAA) through grant NA15NOS4780182.

Acknowledgments

We thank the reviewers for their valuable comments. We thank Dr. Patricia Glibert (Horn point laboratory-UMCES) for valuable comments on the manuscript. This is contribution number ECO1091 from the NOAA ECOHAB program.

Conflict of interest

The authors declare that the research was conducted in the absence of any commercial or financial relationships that could be construed as a potential conflict of interest.

The author(s) declared that they were an editorial board member of Frontiers, at the time of submission. This had no impact on the peer review process and the final decision.

Publisher's note

Supplementary material

The Supplementary Material for this article can be found online at: https://www.frontiersin.org/articles/10.3389/fmars.2024.1305495/full#supplementary-material

References

Adolf, J. E., Bachvaroff, T. R., and Place, A. R. (2009). Environmental modulation of karlotoxin levels in strains of the cosmopolitan dinoflagellate, *Karlodinium veneficum* (Dinophyceae). *J. Phycol.* 45, 176–192. doi: 10.1111/j.1529-8817.2008.00641.x

Adolf, J. E., Krupatkina, D., Bachvaroff, T., and Place, A. R. (2007). Karlotoxin mediates grazing by *Oxyrrhis marina* on strains of *Karlodinium veneficum*. *Harmful Algae* 6, 400–412. doi: 10.1016/j.hal.2006.12.003

Adolf, J. E., Bachvaroff, T., and Place, A. R. (2008). Can cryptophyte abundance trigger toxic karlodinium veneficum blooms in eutrophic estuaries? *Harmful Algae* 8, 119–128. doi: 10.1016/j.hal.2008.08.003

Baker, K. G., Radford, D. T., Evenhuis, C., Kuzhiumparam, U., Ralph, P. J., and Doblin, M. A. (2018). Thermal niche evolution of functional traits in a tropical marine phototroph. *J. Phycol.* 54, 799–810. doi: 10.1111/jpy.12759

Bercel, T. L., and Kranz, S. A. (2019). Insights into carbon acquisition and photosynthesis in *Karenia brevis* under a range of CO_2 concentrations. *Prog. Oceanogr.* 172, 65–76. doi: 10.1016/j.pocean.2019.01.011

Bermúdez, R., Feng, Y., Roleda, M. Y., Tatters, A. O., Hutchins, D. A., Larsen, T., et al. (2015). Long-term conditioning to elevated pCO_2 and warming influences the fatty and amino acid composition of the diatom *Cylindrotheca fusiformis*. *PloS One* 10, 1–15. doi: 10.1371/journal.pone.0123945

Brading, P., Warner, M. E., Davey, P., Smith, D. J., Achterberg, E. P., and Suggett, D. J. (2011). Differential effects of ocean acidification on growth and photosynthesis among phylotypes of *Symbiodinium* (Dinophyceae). *Limnol. Oceanogr.* 56, 927–938. doi: 10.4319/lo.2011.56.3.0927

Brandenburg, K. M., Velthuis, M., and Van de Waal, D. B. (2019). Meta-analysis reveals enhanced growth of marine harmful algae from temperate regions with warming and elevated CO_2 levels. *Glob Change Biol.* 25, 2607–2618. doi: 10.1111/gcb.14678

Brownlee, E. F., Sellner, S. G., Sellner, K. G., Nonogaki, H., Adolf, J. E., Bachvaroff, T. R., et al. (2008). Responses of *Crassostrea virginica* (Gmelin) and *C. ariakensis* (Fujita) to bloom-forming phytoplankton including ichthyotoxic *Karlodinium veneficum* (Ballantine). *J. Shellfish Res.* 27, 581–591. doi: 10.2983/0730-8000(2008)27[581:ROCVGA]2.0.CO;2

Burkhardt, S., Zondervan, I., and Riebesell, U. (1999). Effect of CO_2 concentration on C:N:P ratio in marine phytoplankton: A species comparison. *Limnol. Oceanogr.* 44, 683–690. doi: 10.4319/lo.1999.44.3.0683

Claquin, P., Probert, I., Lefebvre, S., and Veron, B. (2008). Effects of temperature on photosynthetic parameters and TEP production in eight species of marine microalgae. *Aquat. Microb. Ecol.* 51, 1–11. doi: 10.3354/ame01187

Clark, D. R., Flynn, K. J., and Fabian, H. (2014). Variation in elemental stoichiometry of the marine diatom *Thalassiosira weissflogii* (Bacillariophyceae) in response to combined nutrient stress and changes in carbonate chemistry. *J. Phycol.* 50, 640–651. doi: 10.1111/jpy.12208

Collins, S., and Bell, G. (2004). Phenotypic consequences of 1000 generations of selection at elevated CO_2 in a green alga. *Nature* 431, 566–569. doi: 10.1038/nature02945

Collins, S., Boyd, P., and Doblin, M. A. (2020). Evolution, microbes, and changing ocean conditions. *Annu. Rev. Mar. Sci.* 12, 181–208. doi: 10.1146/annurev-marine-010318-095311

Cosgrove, J., and Borowitzka, M. A. (2010). ""Chlorophyll fluorescence terminology: an introduction,"," in *Chlorophyll a Fluorescence in Aquatic Sciences: Methods and Applications*. Eds. D. J. Suggett, O. Prášil and M. A. Borowitzka (Springer Netherlands, Dordrecht), 1–17. doi: 10.1007/978-90-481-9268-7_1

Coyne, K. J., Salvitti, L. R., Mangum, A. M., Ozbay, G., Main, C. R., Kouhanestani, Z. M., et al. (2021). Interactive effects of light, $CO_{2\ and}$ temperature on growth and

resource partitioning by the mixotrophic dinoflagellate, *Karlodinium veneficum*. *PloS One* 16, e0259161. doi: 10.1371/journal.pone.0259161

Cripps, G., Flynn, K. J., and Lindeque, P. K. (2016). Ocean acidification affects the phyto-zoo plankton trophic transfer efficiency. *PloS One* 11, 1–15. doi: 10.1371/journal.pone.0151739

Dayeh, V. R., Schirmer, K., Lee, L. E. J., and Bols, N. C. (2005). ""Rainbow trout gill cell line microplate cytotoxicity test,"," in *Small-scale Freshwater Toxicity Investigations: Toxicity Test Methods*. Eds. C. Blaise and J.-F. Férard (Springer Netherlands, Dordrecht), 473–503. doi: 10.1007/1-4020-3120-3_16

Deeds, J. R., Terlizzi, D. E., Adolf, J. E., Stoecker, D. K., and Place, A. R. (2002). Toxic activity from cultures of *Karlodinium micrum* (=*Gyrodinium galatheanum*) (Dinophyceae) - A dinoflagellate associated with fish mortalities in an estuarine aquaculture facility. *Harmful Algae* 1, 169–189. doi: 10.1016/S1568-9883(02)00027-6

Deng, Y., Wang, K., Hu, Z., Hu, Q., and Tang, Y. Z. (2022). Identification and implications of a core bacterial microbiome in 19 clonal cultures laboratory-reared for months to years of the cosmopolitan dinoflagellate *Karlodinium veneficum*. *Front. Microbiol.* 13. doi: 10.3389/fmicb.2022.967610

DuBois, M., Gilles, K., Hamilton, J. K., Rebers, P. A., and Smith, F. (1951). A colorimetric method for the determination of sugars. *Nature* 168, 167. doi: 10.1038/168167a0

Engel, A., Piontek, J., Grossart, H.-P., Riebesell, U., Schulz, K. G., and Sperling, M. (2014). Impact of CO_2 enrichment on organic matter dynamics during nutrient induced coastal phytoplankton blooms. *J. Plankton Res.* 36, 641–657. doi: 10.1093/plankt/fbt125

Ernst, O., and Zor, T. (2010). Linearization of the bradford protein assay. *J. Vis. Exp.* 38, 1918. doi: 10.3791/1918

Errera, R. M., Yvon-Lewis, S., Kessler, J. D., and Campbell, L. (2014). Reponses of the dinoflagellate *Karenia brevis* to climate change: pCO_2 and sea surface temperatures. *Harmful Algae* 37, 110–116. doi: 10.1016/j.hal.2014.05.012

Eschbach, E., Scharsack, J. P., John, U., and Medlin, L. K. (2001). Improved erythrocyte lysis assay in microtiter plates for sensitive detection and efficient measurement of hemolytic compounds from ichthyotoxic algae. *J. Appl. Toxicol.* 21, 513–519. doi: 10.1002/jat.797

Feng, Y., Warner, M. E., Zhang, Y., Sun, J., Fu, F., Rose, J. M., et al. (2008). Interactive effects of increased pCO_2, temperature and irradiance on the marine coccolithophore *Emiliania huxleyi* (Prymnesiophyceae). *Eur. J. Phycology* 43, 87–98. doi: 10.1080/09670260701664674

Fields, D. M., Runge, J. A., Thompson, C. R. S., Durif, C. M. F., Shema, S. D., Bjelland, R. M., et al. (2022). A positive temperature-dependent effect of elevated CO_2 on growth and lipid accumulation in the planktonic copepod, *Calanus finmarchicus*. *Limnol. Oceanogr.* 68, S87–S100. doi: 10.1002/lno.12261

Fitzer, S. C., Plancq, J., Floyd, C. J., Kemp, F. M., and Toney, J. L. (2019). Increased pCO_2 changes the lipid production in important aquacultural feedstock algae *Isochrysis galbana*, but not in *Tetraselmis suecica*. *Aquac. Fish.* 4, 142–148. doi: 10.1016/j.aaf.2019.02.008

Flores-Moya, A., Rouco, M., García-Sánchez, M. J., García-Balboa, C., González, R., Costas, E., et al. (2012). Effects of adaptation, chance, and history on the evolution of the toxic dinoflagellate *Alexandrium minutum* under selection of increased temperature and acidification. *Ecol. Evol.* 2, 1251–1259. doi: 10.1002/ece3.198

Flynn, K. J., Clark, D. R., Mitra, A., Fabian, H., Hansen, P. J., Glibert, P. M., et al. (2015). Ocean acidification with (de)eutrophication will alter future phytoplankton growth and succession. *Proc. R. Soc B Biol. Sci.* 282, 20142604. doi: 10.1098/rspb.2014.2604

Friedrich, G. E., Walz, P. M., Burczynski, M. G., and Chavez, F. P. (2002). Inorganic carbon in the central California upwelling system during the 1997-1999 El Ninão-La Ninãa event. *Prog. Oceanogr.* 54, 185–203. doi: 10.1016/S0079-6611(02)00049-6

Fu, F. X., Place, A. R., Garcia, N. S., and Hutchins, D. A. (2010). CO_2 and phosphate availability control the toxicity of the harmful bloom dinoflagellate *Karlodinium veneficum*. *Aquat. Microb. Ecol.* 59, 55–65. doi: 10.3354/ame01396

Fu, F. X., Zhang, Y., Warner, M. E., Feng, Y., Sun, J., and Hutchins, D. A. (2008). A comparison of future increased CO_2 and temperature effects on sympatric *Heterosigma akashiwo* and *Prorocentrum minimum*. *Harmful Algae* 7, 76–90. doi: 10.1016/j.hal.2007.05.006

Fuschino, J. R., GusChina, I. A., Dobson, G., Yan, N. D., Harwood, J. L., and Arts, M. T. (2011). Rising water temperatures alter lipid dynamics and reduce n-3 essential fatty acid concentrations in *Scenedesmus obliquus* (chlorophyta). *J. Phycol.* 47, 763–774. doi: 10.1111/jpy.2011.47.issue-4

Glibert, P. M. (2020). Harmful algae at the complex nexus of eutrophication and climate change. *Harmful Algae* 91, 101583. doi: 10.1016/j.hal.2019.03.001

Glibert, P. M., Alexander, J., Meritt, D. W., North, E. W., and Stoecker, D. K. (2007). Harmful algae pose additional challenges for oyster restoration: impacts of the harmful algae *Karlodinium veneficum* and *Prorocentrum minimum* on early life stages of the oysters *Crassostrea virginica* and *Crassostrea ariakensis*. *J. Shellfish Res.* 26, 919–925. doi: 10.2983/0730-8000(2007)26[919:HAPACF]2.0.CO;2

Glibert, P. M., Icarus Allen, J., Artioli, Y., Beusen, A., Bouwman, L., Harle, J., et al. (2014). Vulnerability of coastal ecosystems to changes in harmful algal bloom distribution in response to climate change: projections based on model analysis. *Glob. Change Biol.* 20, 3845–3858. doi: 10.1111/gcb.12662

Gobler, C. J., Doherty, O. M., Hattenrath-Lehmann, T. K., Griffith, A. W., Kang, Y., and Litaker, R. W. (2017). Ocean warming since 1982 has expanded the niche of toxic algal blooms in the North Atlantic and North Pacific oceans. *Proc. Natl. Acad. Sci.* 114, 4975–4980. doi: 10.1073/pnas.1619575114

Gobler, C. J. (2020). Climate change and harmful algal blooms: Insights and perspective. *Harmful Algae.* 91, 101731. doi: 10.1016/j.hal.2019.101731

Guillard, R. R. L., and Ryther, J. H. (1962). Studies of Marine Planktonic Diatoms: I. *Cyclotella nana* Hustedt, and *Detonula confervacea* (Cleve) Gran. *Can. J. Microbiol.* 8, 229–239. doi: 10.1139/m62-029

Hallegraeff, G. M. (2010). Ocean climate change, phytoplankton community responses, and harmful algal blooms: A formidable predictive challenge. *J. Phycol.* 46, 220–235. doi: 10.1111/jpy.2010.46.issue-2

Hattenrath-Lehmann, T. K., Smith, J. L., Wallace, R. B., Merlo, L. R., Koch, F., Mittelsdorf, H., et al. (2015). The effects of elevated CO_2 on the growth and toxicity of field populations and cultures of the saxitoxin-producing dinoflagellate, *Alexandrium fundyense*. *Limnol. Oceanogr.* 60, 198–214. doi: 10.1002/lno.10012

Hennon, G. M. M., Limón, M. D. H., Haley, S. T., Juhl, A. R., Dyhrman, S. T., and Scott, K. (2017). Diverse CO_2 -induced responses in physiology and gene expression among eukaryotic phytoplankton. *Front. Microbiol.* 8. doi: 10.3389/fmicb.2017.02547

Hennon, G. M. M., Morris, J. J., Haley, S. T., Zinser, E. R., Durrant, A. R., Entwistle, E., et al. (2018). The impact of elevated CO_2 on *Prochlorococcus* and microbial interactions with 'helper' bacterium Alteromonas. *ISME J.* 12, 520–531. doi: 10.1038/ismej.2017.189

Hixson, S. M., and Arts, M. T. (2016). Climate warming is predicted to reduce omega-3, long-chain, polyunsaturated fatty acid production in phytoplankton. *Glob Chang Biol.* 22 (8), 2744–2755. doi: 10.1111/gcb.13295

Hong, H., Talapatra, S., Katz, J., Tester, P. A., Waggett, R. J., and Place, A. R. (2012). Algal toxins alter copepod feeding behavior. *PloS One* 7, e36845. doi: 10.1371/journal.pone.0036845

Hyun, B., Ju, S. J., Ko, A. R., Choi, K. H., Jung, S. W., Jang, P. G., et al. (2016). Thermal effects on the growth and fatty acid composition of four harmful algal bloom species: Possible implications for ichthyotoxicity. *Ocean Sci. J.* 51, 333–342. doi: 10.1007/s12601-016-0029-5

IPCC (2014). "Climate change 2014: synthesis report," in *Contribution of Working Groups I, II and III to the Fifth Assessment Report of the Intergovernmental Panel on Climate Change*. Eds. R. K. Pachauri and L. A. Meyer (IPCC, Geneva, Switzerland), 151. Core Writing Team.

IPCC (2021). "Summary for policymakers," in *Climate Change 2021: The Physical Science Basis. Contribution of Working Group I to the Sixth Assessment Report of the Intergovernmental Panel on Climate Change*. Eds. V. Masson-Delmotte, P. Zhai, A. Pirani, S. L. Connors, C. Péan, S. Berger, et al. (Cambridge University Press, Cambridge, United Kingdom and New York, NY, USA), 3–32. doi: 10.1017/9781009157896.001

Jacob, B. G., Dassow, P. V. O. N., Salisbury, J. E., Navarro, J. M., and Vargas, C. A. (2017). Impact of low pH/high pCO_2 on the physiological response and fatty acid content in diatom *Skeletonema pseudocostatum*. *J. Mar. Biol. Assoc.* 97, 225–233. doi: 10.1017/S0025315416001570

Jin, P., Gonzàlez, G., and Agustí, S. (2020). Long-term exposure to increasing temperature can offset predicted losses in marine food quality (fatty acids) caused by ocean warming. *Evol. Appl.* 13, 2497–2506. doi: 10.1111/eva.13059

Jin, P., Ji, Y., Huang, Q., Li, P., Pan, J., Lu, H., et al. (2022). A reduction in metabolism explains the tradeoffs associated with the long-term adaptation of phytoplankton to high CO_2 concentrations. *New Phytol.* 233, 2155–2167. doi: 10.1111/nph.17917

Johnson, M. D., Rome, M., and Stoecker, D. K. (2003). Microzooplankton grazing on *Prorocentrum minimum* and *Karlodinium micrum* in Chesapeake Bay. *Limnol. Oceanogr.* 48, 238–248. doi: 10.4319/lo.2003.48.1.0238

Jónasdóttir, S. H., Visser, A. W., and Jespersen, C. (2009). Assessing the role of food quality in the production and hatching of *Temora longicornis* eggs. *Mar. Ecol. Prog. Ser.* 382, 139–150. doi: 10.3354/meps07985

Kremp, A., Godhe, A., Egardt, J., Dupont, S., Suikkanen, S., Casabianca, S., et al. (2012). Intraspecific variability in the response of bloom-forming marine microalgae to changed climate conditions. *Ecol. Evol.* 2, 1195–1207. doi: 10.1002/ece3.245

Le Bescot, N., Mahé, F., Audic, S., Dimier, C., Garet, M.-J., Poulain, J., et al. (2016). Global patterns of pelagic dinoflagellate diversity across protist size classes unveiled by metabarcoding. *Environ. Microbiol.* 18, 609–626. doi: 10.1111/1462-2920.13039

Li, A., Stoecker, D. K., and Coats, D. W. (2001). Use of the 'Food vacuole content' method to estimate grazing by the mixotrophic dinoflagellate gyrodinium galatheanum on cryptophytes. *J. Plankton Res.* 23, 303–318. doi: 10.1093/plankt/23.3.303

Li, J., Glibert, P. M., and Gao, Y. (2015). Temporal and spatial changes in Chesapeake Bay water quality and relationships to *Prorocentrum minimum*, *Karlodinium veneficum*, and CyanoHAB events 1991-2008. *Harmful Algae* 42, 1–14. doi: 10.1016/j.hal.2014.11.003

Li, M., Chen, Y., Zhang, F., Song, Y., Glibert, P. M., and Stoecker, D. K. (2022). A three-dimensional mixotrophic model of *Karlodinium veneficum* blooms for a eutrophic estuary. *Harmful Algae* 113, 102203. doi: 10.1016/j.hal.2022.102203

Lin, C.-H., Flynn, K. J., Mitra, A., and Glibert, P. M. (2018). Simulating effects of variable stoichiometry and temperature on mixotrophy in the harmful dinoflagellate karlodinium veneficum. *Front. Mar. Sci.* 5. doi: 10.3389/fmars.2018.00320

Lohbeck, K. T., Riebesell, U., and Reusch, T. B. H. (2012). Adaptive evolution of a key phytoplankton species to ocean acidification. *Nat. Geosci.* 5, 346–351. doi: 10.1038/ngeo1441

MacIntyre, H. L., and Cullen, J. J. (2005). "Using cultures to investigate the physiological ecology of microalgae," in *Algal Culturing Techniques*. Ed. R. Andersen (Elsevier Academic Press), 287–326.

McLaskey, A. K., Keister, J. E., Schoo, K. L., Olson, M. B., and Love, B. A. (2019). Direct and indirect effects of elevated CO_2 are revealed through shifts in phytoplankton, copepod development, and fatty acid accumulation. *PloS One* 14, e0213931. doi: 10.1371/journal.pone.0213931

Meyers, M. T., Cochlan, W. P., Carpenter, E. J., and Kimmerer, W. J. (2019). Effect of ocean acidification on the nutritional quality of marine phytoplankton for copepod reproduction. *PloS One* 14. doi: 10.1371/journal.pone.0217047

Meyers, M., Décima, M., Law, C. S., Gall, M., Barr, N., Miller, M. R., et al. (2022). No evidence of altered relationship between diet and consumer fatty acid composition in a natural plankton community under combined climate drivers. *J. Exp. Mar. Bio. Ecol.* 551. doi: 10.1016/j.jembe.2022.151734

Nielsen, L. T., Jakobsen, H. H., and Hansen, P. J. (2010). High resilience of two coastal plankton communities to twenty-first century seawater acidification: Evidence from microcosm studies. *Mar. Biol. Res.* 6, 542–555. doi: 10.1080/17451000903476941

O'Donnell, D. R., Du, Z., and Litchman, E. (2019). Experimental evolution of phytoplankton fatty acid thermal reaction norms. *Evol. Appl.* 12, 1201–1211. doi: 10.1111/eva.12798

Pan, Y., Meng, R., Li, Y., Yang, L., Mei, L., Wu, Y., et al. (2023). Changes in biochemical metabolites in manila clam after a temporary culture with high-quality microalgal feed mixed with the dinoflagellate species *Karlodinium veneficum* and *K. zhouanum*. *Harmful Algae* 125, 102422. doi: 10.1016/j.hal.2023.102422

Passow, U., and Laws, E. A. (2015). Ocean acidification as one of multiple stressors: growth response of *Thalassiosira weissflogii* (diatom) under temperature and light stress. *Mar. Ecol. Prog. Ser.* 541, 75–90. doi: 10.3354/meps11541

Pierrot, D., Lewis, E., and Wallace, D. (2006). *MS Excel program developed for CO2 system calculations* (Oak Ridge Oak Ridge Natl. Lab. Dioxide Inf. Anal. Cent). Available at: http://cdiac.ornl.gov/oceans/co2rprt.html.

Place, A. R., Bowers, H. A., Bachvaroff, T. R., Adolf, J. E., Deeds, J. R., and Sheng, J. (2012). *Karlodinium veneficum*-The little dinoflagellate with a big bite. *Harmful Algae* 14, 179–195. doi: 10.1016/j.hal.2011.10.021

R Core Team (2021). *R: A language and environment for statistical computing* (Vienna, Austria: R Foundation for Statistical Computing). Available at: https://www.R-project.org/.

Rossoll, D., Bermúdez, R., Hauss, H., Schulz, K. G., Riebesell, U., Sommer, U., et al. (2012). Ocean acidification-induced food quality deterioration constrains trophic transfer. *PloS One* 7, e34737. doi: 10.1371/journal.pone.0034737

Sato, N., Tsuzuki, M., and Kawaguchi, A. (2003). Glycerolipid synthesis in *Chlorella kessleri* 11h - II. 1633 (1), 35–42. doi: 10.1016/S1388-1981(03)00070-2

Schlüter, L., Lohbeck, K. T., Gröger, J. P., Riebesell, U., and Reusch, T. B. (2016). Long-term dynamics of adaptive evolution in a globally important phytoplankton species to ocean acidification. *Sci. Adv.* 2, e1501660. doi: 10.1126/sciadv.1501660

Schlüter, L., Lohbeck, K. T., Gutowska, M. A., Gröger, J. P., Riebesell, U., and Reusch, T. B. H. (2014). Adaptation of a globally important coccolithophore to ocean warming and acidification. *Nat. Clim. Change* 4, 1024–1030. doi: 10.1038/nclimate2379

Seto, D. S., Karp-Boss, L., and Wells, M. L. (2019). Effects of increasing temperature and acidification on the growth and competitive success of *Alexandrium catenella* from the Gulf of Maine. *Harmful Algae* 89, 101670. doi: 10.1016/j.hal.2019.101670

Sheppard, A. J. (1992). *Lipid manual: Methodology suitable for fatty acid-cholesterol analysis* (Dubuque, Iowa: Wm. C. Brown Publishers).

Sinensky, M. (1974). Homeoviscous adaptation–a homeostatic process that regulates the viscosity of membrane lipids in *Escherichia coli*. *Proc. Natl. Acad. Sci.* 71, 522–525. doi: 10.1073/pnas.71.2.522

Solórzano, L., and Sharp, J. H. (1980). Determination of total dissolved phosphorus and particulate phosphorus in natural waters1. *Limnol. Oceanogr.* 25, 754–758. doi: 10.4319/lo.1980.25.4.0754

Stoecker, D. K., Adolf, J. E., Place, A. R., Glibert, P. M., and Meritt, D. W. (2008). Effects of the dinoflagellates *Karlodinium veneficum* and *Prorocentrum minimum* on early life history stages of the eastern oyster (*Crassostrea virginica*). *Mar. Biol.* 154, 81–90. doi: 10.1007/s00227-007-0901-z

Sugie, K., and Yoshimura, T. (2016). Effects of high CO_2 levels on the ecophysiology of the diatom *Thalassiosira weissflogii* differ depending on the iron nutritional status. *ICES J. Mar. Sci.* 73, 680–692. doi: 10.1093/icesjms/fsv259

Tatters, A. O., Flewelling, L. J., Fu, F., Granholm, A. A., and Hutchins, D. A. (2013a). High CO_2 promotes the production of paralytic shellfish poisoning toxins by *Alexandrium catenella* from Southern California waters. *Harmful Algae* 30, 37–43. doi: 10.1016/j.hal.2013.08.007

Tatters, A. O., Roleda, M. Y., Schnetzer, A., Fu, F., Hurd, C. L., Boyd, P. W., et al. (2013b). Short- and long-term conditioning of a temperate marine diatom community to acidification and warming. *Philos. Trans. R. Soc B Biol. Sci.* 368, 20120437. doi: 10.1098/rstb.2012.0437

Taucher, J., Haunost, M., Boxhammer, T., Bach, L. T., Algueró-Muñiz, M., and Riebesell, U. (2017). Influence of ocean acidification on plankton community structure during a winter-to summer succession: An imaging approach indicates that copepods can benefit from elevated CO_2 via indirect food web effects. *PloS One* 12, e0169737. doi: 10.1371/journal.pone.0169737

Torstensson, A., Hedblom, M., Andersson, J., Andersson, M. X., and Wulff, A. (2013). Synergism between elevated pCO_2 and temperature on the Antarctic sea ice diatom *Nitzschia lecointei*. *Biogeosciences* 10, 6391–6401. doi: 10.5194/bg-10-6391-2013

Trainer, V. L., Moore, S. K., Hallegraeff, G., Kudela, R. M., Clement, A., Mardones, J. I., et al. (2019). Pelagic harmful algal blooms and climate change: Lessons from nature's experiments with extremes. *Harmful Algae* 91, 101591. doi: 10.1016/j.hal.2019.03.009

Van Wychen, S., Ramirez, K., and Laurens, L. M. L. (2013). *Determination of Total Lipids as Fatty Acid Methyl Esters (FAME) by in* situ *Transesterification: Laboratory Analytical Procedure (LAP)* (Golden, CO: National Renewable Energy Laboratory). NREL/TP-2700-87501

Vidyarathna, N. K., Ahn, S.H.(., and Glibert, P. M. (2023). Thermal niche of the dinoflagellate *Karlodinium veneficum* across different salinity and light levels. *J. Plankton Res.* 45 (4), 604–613, fbad019. doi: 10.1093/plankt/fbad019

Vidyarathna, N. K., Papke, E., Coyne, K. J., Cohen, J. H., and Warner, M. E. (2020). Functional trait thermal acclimation differs across three species of mid-Atlantic harmful algae. *Harmful Algae* 94, 101804. doi: 10.1016/j.hal.2020.101804

Waggett, R. J., Tester, P. A., and Place, A. R. (2008). Anti-grazing properties of the toxic dinoflagellate *Karlodinium veneficum* during predator-prey interactions with the copepod *Acartia tonsa*. *Mar. Ecol. Prog. Ser.* 366, 31–42. doi: 10.3354/meps07518

Wang, T., Tong, S., Liu, N., Li, F., Wells, M. L., and Gao, K. (2017). The fatty acid content of plankton is changing in subtropical coastal waters as a result of OA: Results from a mesocosm study. *Mar. Environ. Res.* 132, 51–62. doi: 10.1016/j.marenvres.2017.10.010

Wells, M. L., Trainer, V. L., Smayda, T. J., Karlson, B. S. O., Trick, C. G., Kudela, R. M., et al. (2015). Harmful algal blooms and climate change: Learning from the past and present to forecast the future. *Harmful Algae* 49, 68–93. doi: 10.1016/j.hal.2015.07.009

Welschmeyer, N. A. (1994). Fluorometric analysis of chlorophyll a in the presence of chlorophyll b and pheopigments. *Limnol. Oceanogr.* 39, 1985–1992. doi: 10.4319/lo.1994.39.8.1985

Wilken, S., Huisman, J., Naus-Wiezer, S., and Van Donk, E. (2013). Mixotrophic organisms become more heterotrophic with rising temperature. *Ecol. Lett.* 16, 225–233. doi: 10.1111/ele.12033

Wynn-Edwards, C., King, R., Davidson, A., Wright, S., Nichols, P. D., Wotherspoon, S., et al. (2014). Species-specific variations in the nutritional quality of Southern Ocean phytoplankton in response to elevated pCO_2. *Water* 6, 1840–1859. doi: 10.3390/w6061840

Xu, D., Zheng, G., Brennan, G., Wang, Z., Jiang, T., Sun, K., et al. (2023). Plastic responses lead to increased neurotoxin production in the diatom *Pseudo-nitzschia* under ocean warming and acidification. *ISME J.* 17, 525–536. doi: 10.1038/s41396-023-01370-8

Yao, W., and Byrne, R. H. (1998). Simplified seawater alkalinity analysis: Use of linear array spectrometers. *Deep Sea Res. Part I Oceanogr. Res. Pap.* 45, 1383–1392. doi: 10.1016/S0967-0637(98)00018-1

Zhang, H., Litaker, W., Vandersea, M. W., Tester, P., and Lin, S. (2008). Geographic distribution of Karlodinium veneficum in the US east coast as detected by ITS–ferredoxin real-time PCR assay. *J. Plankton Res.* 30, 905–922. doi: 10.1093/plankt/fbn047